

Room-temperature 2.5 μm InGaAsSb/AlGaAsSb diode lasers emitting 1 W continuous waves

J. G. Kim

Sarnoff Corporation, CN5300, Princeton, New Jersey 08543-5300

L. Shterengas^{a)}

Department of Electrical and Computer Engineering, State University of New York at Stony Brook, Stony Brook, New York 11794-2350

R. U. Martinelli

Sarnoff Corporation, CN5300, Princeton, New Jersey 08543-5300

G. L. Belenky

Department of Electrical and Computer Engineering, State University of New York at Stony Brook, Stony Brook, New York 11794-2350

D. Z. Garbuzov

Princeton Lightwave, Inc., Cranbury, New Jersey 08512

W. K. Chan

Sarnoff Corporation, CN5300, Princeton, New Jersey 08543-5300

(Received 24 June 2002; accepted 4 September 2002)

We have characterized 2.5- μm -wavelength InGaAsSb/AlGaAsSb/GaSb two-quantum-well diode lasers that emit 1 W continuous waves from a 100- μm -wide aperture at a temperature of 12 °C. The threshold current density is 250 A/cm², and the external quantum efficiency near threshold is 0.36. The wall-plug efficiency reaches a maximum of 12% at a current of 2 A. Operating in the pulsed-current mode, the devices output nearly 5 W at 20 °C. These lasers exhibit internal losses of about 4 cm⁻¹ and differential series resistances of about 0.1 Ω . A broad-waveguide design lowers internal losses, and highly doped transition regions between the cladding layers and the GaSb reduces series resistance. © 2002 American Institute of Physics. [DOI: 10.1063/1.1517176]

High-power midinfrared diode lasers operating at room temperature have important applications in countermeasures, LIDAR, remote trace-gas monitoring, and secure communications. Recent work extended room-temperature operation of antimonide-based devices to a wavelength of 2.7 μm .¹ The devices incorporated two 20-nm-wide “quasiternary” InGaAsSb quantum wells (QWs) surrounded by Al_{0.3}Ga_{0.7}As_{0.03}Sb_{0.97} barriers and separate-heterostructure-confinement (SCH) layers. (The quantum-well material is called quasiternary because of its low As content.) The maximum cw output power at 17 °C for a 2.5- μm -wavelength device was 250 mW. The threshold current density was about 300 A/cm², and the external quantum efficiency, η_d , was 0.30.¹ We have redesigned the laser structure to reduce internal loss, α_i ,² and series resistance. The two QWs in our devices are 14.5-nm-wide In_{0.41}Ga_{0.59}As_{0.14}Sb_{0.86} quaternaries. The barriers and SCH layers are Al_{0.25}Ga_{0.75}As_{0.02}Sb_{0.98}. These design changes produced internal losses of 4 cm⁻¹, and, coupled with the devices’ low series resistance of 0.1 Ω that reduces power dissipation, the devices output considerably more power. We have measured maximum continuous-wave output powers of 1 W at 12 °C with η_d values of 0.36. In the pulsed-current mode the peak power at 20 °C was nearly 5 W.

Figure 1 schematically depicts the energy bands of the broadened-waveguide (BW) two QW 2.5 μm InGaAsSb/

AlGaAsSb diode laser. The devices were grown by molecular-beam epitaxy (MBE). Heavily doped, compositionally graded, 40-nm-thick regions between the cladding layers and the n -GaSb substrate and the p^+ -GaSb cap layer improve electron and hole conduction. The n region is Te doped to 1×10^{18} cm⁻³ and the p region is Be doped to 2×10^{19} cm⁻³. The cladding layers are 2- μm -thick Al_{0.9}Ga_{0.1}As_{0.07}Sb_{0.93}. The n -cladding layer is Te doped to 3×10^{17} cm⁻³, and the p -cladding layer is Be doped to 1×10^{18} cm⁻³ over the first 0.2 μm and to 5×10^{18} cm⁻³ over the remaining 1.8 μm . This was done to reduce intervalence-band absorption.² The undoped SCH- and barrier-layer composition is Al_{0.25}Ga_{0.75}As_{0.02}Sb_{0.98}. The two In_{0.41}Ga_{0.59}As_{0.14}Sb_{0.86} QWs are 14.5 nm wide. They are 1.6% compressively strained. The calculated type-I band off-

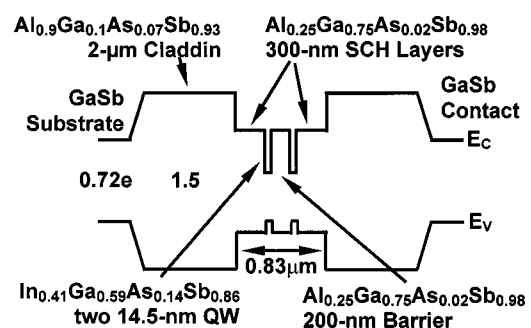


FIG. 1. Schematic energy-band diagram of the 2.5 μm diode laser.

^{a)}Electronic mail: leon@ece.sunysb.edu

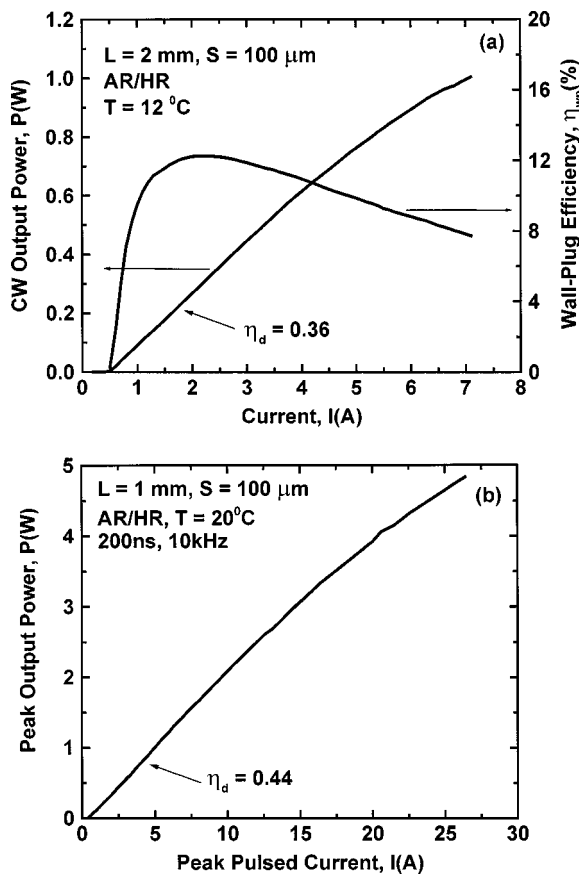


FIG. 2. Output characteristics of two 2.5 μm diode lasers in the cw (a) and pulsed-current mode (b). The output aperture, cavity length, and the heatsink temperature are indicated in each graph.

sets for the QWs are 0.139 eV in the valence band and 0.336 eV in the conduction band. The wafers were processed into 100-μm-aperture lasers with antireflection (AR) and high-reflection (HR) facet coatings of 3% and 95% reflectivity, respectively. Cavity lengths are 1 and 2 mm. The devices were indium-soldered *p*-side down to copper mounts and characterized.

Figures 2(a) and 2(b) show the cw and pulsed-mode (200 ns current pulses at a 10 kHz repetition rate) output-power (*P*–*I*) characteristics of 2 and 1-mm-long diode lasers, respectively. The wall–plug efficiency for cw operation is shown in Fig. 2(a). The cw threshold current, I_{th} , is 0.5 A (250 A/cm²), and near threshold η_d is 0.36 photons/electron. With increasing current the power tends to saturate as a result of heating, and the maximum power is 1 W at a heatsink temperature of 12 °C. The peak wall–plug efficiency of 12% occurs at a current of about 2 A. Active-area heating is not as significant a problem in pulsed-mode operation. Figure 2(b) shows that at a heatsink temperature of 20 °C a 1-mm-long device outputs a maximum peak power of 4.9 W at 27 A, which is power-supply limited. The shorter cavity length of 1 mm increases η_d to 0.44, because of the higher mirror losses.

Figure 3 shows the characteristic temperatures, T_0 and T_1 , associated with the exponential change in I_{th} and external slope efficiency, η_s ($\eta_d = 2[A/W]\eta_s$), measured in pulsed-current operation over the temperature range of 20–60 °C. We found $T_0 = 83$ K and $T_1 = 185$ K over the temperature range of 20–60 °C. Over the limited temperature range of 20–40 °C, $T_0 = 89$ K and $T_1 = 251$ K. These

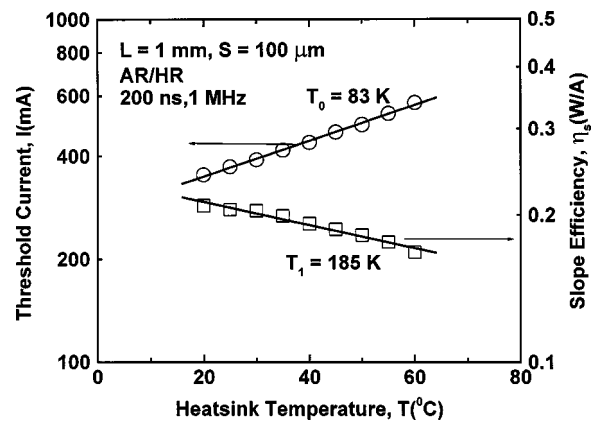


FIG. 3. Characteristic temperatures, T_0 and T_1 , for a 1-mm-long, 2.5 μm diode laser.

latter values are comparable to those of 2.3 μm antimonide lasers.¹ Characteristic temperatures generally decrease with increasing wavelength for antimonide diode lasers.

Figure 4 shows the cw spectra at 15, 23, and 30 °C, all taken at a current of 1 A. The spectra are multimode, and at 30 °C the maximum wavelength is 2.508 μm. The long-wavelength edge of the spectrum increases at a rate of 1.5 nm/K, as expected for antimonide-based midinfrared lasers.³

Figure 5 shows the subthreshold modal gain spectra taken at six different currents, for a 1-mm-long laser at 20 SDC. We used the Hakki–Paoli method to obtain these data from the amplified spontaneous emission spectrum at each specified current.^{4,5} For photon energies about 0.47 eV the spectra converge, for the material gain at sub-band-gap energies, is zero at any current and modal gain is equal to total loss ~ 22 cm⁻¹. Subtracting from this value the mirror losses, which are about 18 cm⁻¹ for a 1-mm-long laser, leaves a value for internal loss of 4 cm⁻¹. This value is comparable with the losses in a 2 μm, BW antimonide laser.² Using the measured values of the η_d for 1- and 2-mm-long lasers, we find a consistent value for the internal quantum efficiency, η_i , of about 0.5. Deriving α_i and η_i from a plot of $1/\eta_d$ versus cavity length yield values of ~ 5.2 cm⁻¹ and 0.56, respectively, which are in fair agreement with the numbers obtained from the gain spectra of Fig. 5. BW lasers have lower internal efficiency,² owing perhaps to carrier recombination in the extended SCH layers. We are currently rede-

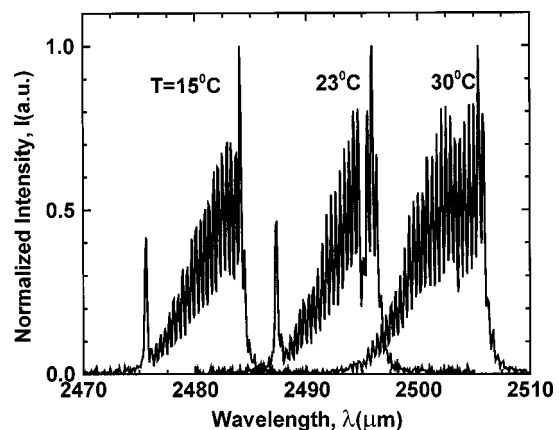


FIG. 4. Cw laser spectra at 15, 23, and 30 °C. $S = 100$ μm, $L = 2$ mm, and $I = 1$ A.

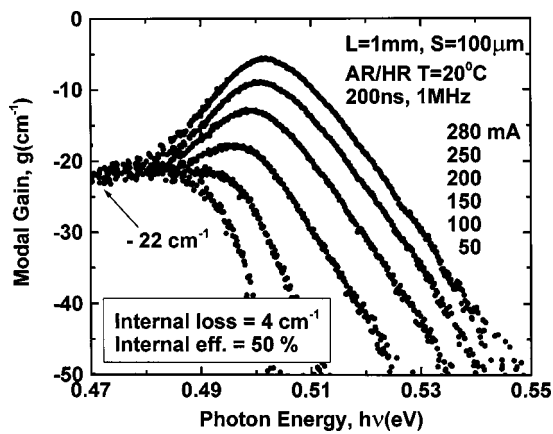


FIG. 5. Six subthreshold gain spectra of a 1-mm-long, $2.5 \mu\text{m}$ diode laser at 20°C . Each gain spectrum was taken at a given current, increasing gain corresponding to increasing current.

signing the waveguide region to check this hypothesis.

To minimize the optical loss, the broadened waveguide laser design was used with total waveguide width $W = 830 \text{ nm}$. The BW approach reduced overlap of the optical field with doped cladding layers to 30%–35% keeping QW confinement of about 3%. The high quality of the MBE-grown materials also produces a low-loss waveguide and enhances laser internal efficiency.

While low internal loss increases external quantum efficiency, it is the low series resistance, R_S , and hence, the low forward voltage of these devices, that enables the relatively high cw output powers. Typically, the forward voltage is 1.6 V at 8 A, and above the turn-on voltage of 0.6 V, we measure R_S values of about 0.1Ω . This is only a factor of 4 greater than the $R_S = 0.026 \Omega$ measured for 980 nm, GaAs-based

diode lasers.⁶ This relatively low series resistance results mainly from the low n -metal contact resistance and the heavily n -doped graded region between the n -cladding layer and the substrate.

In conclusion, we have developed $2.5 \mu\text{m}$ InGaAsSb/AlGaAsSb/GaSb diode lasers with internal losses of 4 cm^{-1} and series resistances of 0.1Ω . These features enable continuous-wave output powers of 1 W at 12°C and pulsed-current mode output powers of 5 W at 20°C . The low internal losses are the result of a strongly mode-confining waveguide. We attribute the low series resistance of 0.1Ω to high doping in the graded layers, including the cladding layers at the graded-layer/cladding-layer interface. We are currently investigating waveguide designs that increase the internal quantum efficiency.

The authors thank Dr. H. Mohseni for technical discussions. The authors also acknowledge the support from the United States Air Force Office of Scientific Research, Grant No. F-49620-01-10108, and from the Air Force Research Laboratory, Directed Energy Directorate, Contract No. F29601-00-C-0003.

¹D. Z. Garbuzov, H. Lee, V. Khalfin, R. Martinelli, J. C. Connolly, and G. L. Belenky, *IEEE Photonics Technol. Lett.* **11**, 794 (1999).

²D. Z. Garbuzov, R. U. Martinelli, H. Lee, P. K. York, R. J. Menna, J. C. Connolly, and S. Y. Narayan, *Appl. Phys. Lett.* **69**, 2006 (1996).

³H. K. Choi, S. J. Eglash, and G. W. Turner, *Appl. Phys. Lett.* **64**, 2474 (1994).

⁴B. W. Hakki and T. L. Paoli, *J. Appl. Phys.* **44**, 4113 (1973).

⁵D. V. Donetsky, G. L. Belenky, D. Z. Garbuzov, H. Lee, R. U. Martinelli, G. Taylor, S. Luryi, and J. C. Connolly, *IEEE Electron Device Lett.* **35**, 298 (1999).

⁶A. Al-Muhanna, L. J. Mawst, D. Botez, D. Z. Garbuzov, R. U. Martinelli, and J. C. Connolly, *Appl. Phys. Lett.* **73**, 1182 (1998).